JCI insight

Short-term overnutrition induces white adipose tissue insulin resistance through *sn*-1,2-diacylglycerol – PKCε – insulin receptor^{T1160} phosphorylation

Kun Lyu, … , Varman T. Samuel, Gerald I. Shulman

JCI Insight. 2021. https://doi.org/10.1172/jci.insight.139946.

Research In-Press Preview Endocrinology Metabolism

Graphical abstract

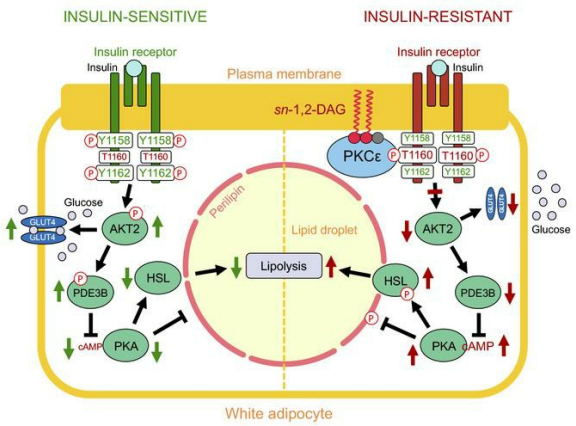

Find the latest version:

https://jci.me/139946/pdf

Short-term overnutrition induces white adipose tissue insulin resistance through *sn*-1,2-diacylglycerol – PKCε – insulin receptor^{T1160} phosphorylation

Kun Lyu[1,2], Dongyan Zhang[1], Joongyu Song[1], Xiruo Li[1,2],

Rachel J. Perry[1,2], Varman T. Samuel[1,3], Gerald I. Shulman[1,2,+]

[1]*Department of Internal Medicine*
[2]*Department of Cellular & Molecular Physiology*
Yale School of Medicine, New Haven, CT 06510, USA
[3]*VA Connecticut Healthcare System, West Haven, CT 06516, USA*

[+]Corresponding author: gerald.shulman@yale.edu

Complete correspondence information:

Mailing address for all authors:
333 Cedar St
P.O. Box 208020
New Haven, CT 06520-8020, USA
Phone: (203) 785-5447

Email address for each author:
1. Kun Lyu: kun.lyu@yale.edu
2. Dongyan Zhang: dongyan.zhang@yale.edu
3. Joongyu D Song: joongyusong@gmail.com
4. Xiruo Li: xiruo.li@yale.edu
5. Rachel J. Perry: rachel.perry@yale.edu
6. Varman T Samuel: varman.samuel@yale.edu
7. Gerald Shulman: gerald.shulman@yale.edu

Abstract

Insulin-mediated suppression of white adipose tissue (WAT) lipolysis is an important anabolic function that is dysregulated in states of overnutrition. However, the mechanism of short-term high-fat diet (HFD)-induced WAT insulin resistance is poorly understood. Based on our recent studies we hypothesize that a short-term HFD causes WAT insulin resistance through increases in plasma membrane (PM) *sn*-1,2-diacylglycerols (DAG), which promotes protein kinase C-ε (PKCε) activation to impair insulin signaling by phosphorylating insulin receptor (Insr) Thr^{1160}. To test this hypothesis, we assessed WAT insulin action in 7-day HFD-fed versus regular chow diet-fed rats during a hyperinsulinemic-euglycemic clamp. HFD feeding caused WAT insulin resistance, reflected by reductions in both insulin-mediated WAT glucose uptake and suppression of WAT lipolysis. These changes were specifically associated with increased PM *sn*-1,2-diacylglycerol (DAG) content, increased PKCε activation and impaired insulin-stimulated $Insr^{Y1162}$ phosphorylation. In order to examine the role of $Insr^{T1160}$ phosphorylation in mediating lipid-induced WAT insulin resistance, we examined these same parameters in short-term HFD-fed $Insr^{T1150A}$ knockin mice (mouse homolog for human Thr^{1160}). Similar to the rat study HFD feeding induced WAT insulin resistance in WT control mice but failed to induce WAT insulin resistance in $Insr^{T1150A}$ mice. Taken together these data demonstrate that the PM *sn*-1,2-DAG - PKCε - $Insr^{T1160}$ phosphorylation pathway plays an important role in mediating lipid-induced WAT insulin resistance and represents a potential therapeutic target to improve insulin sensitivity in WAT.

Introduction

Obesity-related metabolic diseases such as type 2 diabetes and metabolic-associated fatty liver disease (MAFLD) are often accompanied by white adipose tissue (WAT) dysfunction (1, 2). One aspect of WAT dysfunction is WAT insulin resistance, which is partially characterized by insulin's reduced ability to suppress lipolysis, resulting in higher rates of fatty acid delivery to liver and skeletal muscle (1, 3). Ectopic lipid accumulation in insulin-responsive tissues such as liver and skeletal muscle leads to insulin resistance via the accumulation of diacylglycerol (DAG) in the plasma membranes and subsequent translocation and activation of novel PKCs (nPKCs)(1, 4, 5). Accumulation of *sn*-1,2-DAGs in the plasma membrane (PM) activates PKCε which then phosphorylates insulin receptor (Insr) at Thr^{1160} to impair Insr kinase (IRK) autophosphorylation/activation and subsequent activation of downstream signaling events (1, 5-7). This simple model can explain the development of lipid-induced liver and muscle insulin resistance in obese rodents and humans (1, 4-10) as well as the mechanism by which weight loss (11), adiponectin (12), and liver-targeted mitochondrial uncouplers reverse insulin resistance in HFD-fed obese (13, 14) and lipodystrophic (15) insulin resistant rodents.

The pathogenesis of WAT insulin resistance remains unclear. Multiple factors have already been implicated, including low-grade inflammation, altered adipokine secretion and hypoxia (16-18). However, further studies have suggested that WAT insulin resistance can develop early following overfeeding and as a primary event. Additionally, overfed human subjects can develop peripheral insulin resistance prior to WAT immune cell infiltration (19, 20).

Similar to its critical role in lipid-induced hepatic insulin resistance, PKCε also appears to be important in the pathogenesis of WAT insulin resistance. Silencing of both hepatic and WAT PKCε with an antisense oligonucleotide improved WAT insulin action, reflected by increased insulin-stimulated WAT glucose uptake in high-fat diet (HFD)-fed rats (5). Consistent with these results, Brandon and colleagues recently demonstrated improvement of glucose tolerance in HFD-fed WAT-specific PKCε knockout mice (21). However, they did not document any alterations in the WAT insulin signaling pathway or in insulin suppression of WAT lipolysis in these mice (21). Furthermore, there was no conclusion on whether the DAG-PKCε-Insr Thr^{1160} pathway was involved in WAT insulin action regulation or whether another distinct molecular pathway is regulated by PKCε activation to impact glucose tolerance. In this study, we examine the hypothesis that the DAG-PKCε-Insr Thr^{1160} pathway maybe an early contributor to short-term HFD-induced WAT insulin resistance and hinder the ability of insulin to suppress WAT lipolysis and promote WAT glucose uptake, which is necessary for fatty acid esterification into triglyceride.

In order to test this hypothesis, we first explored this pathway in male Sprague Dawley rats fed with HFD versus regular chow diet (RC) for 7 days, a time frame in which fat feeding may induce WAT insulin resistance without causing WAT inflammation in rats (22). We measured the content of DAG stereoisomers in 5 different subcellular compartments – plasma membrane (PM), endoplasmic reticulum (ER), mitochondria (Mito), cytosol and lipid droplet (LD), assayed the translocation of different PKCs and the activation of key steps of the insulin signaling pathway. We further quantified the impact of WAT insulin resistance with a hyperinsulinemic-euglycemic

clamp (HEC) study, using a combination of stable and radiolabeled isotope tracers to measure the alterations in whole body and WAT fatty acid flux and glucose metabolism. Furthermore, to determine whether phosphorylation of Insr Thr^{1160} is necessary for lipid-induced WAT insulin resistance, we performed the same HEC with stable and radiolabeled isotope tracers in WT versus $Insr^{T1150A}$ knockin mice on HFD to assess their WAT insulin sensitivity using these same methods.

Results

Seven-day HFD causes WAT insulin resistance

We performed a HEC combined with [$^{2}H_{7}$]glucose, [$^{2}H_{5}$]glycerol and [$^{13}C_{16}$]palmitate infusions in male Sprague-Dawley rats fed either regular chow (RC) or a 7-day HFD. There was no significant difference in body weight, fasting plasma glucose and insulin concentrations between the RC and HFD group (Table S1). We quantified fatty acid and glycerol turnover in the basal (fasted) state and 30 min after a primed (25 mU/kg-min x 5 min), continuous (2.5 mU/kg-min) insulin infusion. This short HEC clamp was sufficient to establish a steady state in fatty acid and glycerol turnover (Figure S1, E and F), and allowed us to focus on changes in insulin action and signaling linked to the suppression of WAT lipolysis. There were no significant differences in fasting non-esterified fatty acids (NEFA) concentrations or rates of whole-body lipolysis between the groups (Figure 1, A, C and E). However, after 7-day HFD, the ability of insulin to suppress WAT lipolysis was impaired, and we observed less suppression of NEFA concentration (76±3% vs 54±6%, $p<0.001$). Consistent with these results we found that insulin suppression of whole-body glycerol turnover (46±5% vs 23±4%, $p<0.01$) and fatty acid turnover (37±2% vs 23±3%, $p<0.001$) during the HEC clamp were also impaired with 7-day HFD feeding (Figure 1, A-D; Figure S1, C and D). Further, we performed a 140-min HEC to quantify insulin-stimulated glucose uptake in WAT. Rats fed a 7-day HFD exhibit a ~50% reduction in WAT glucose uptake (Figure 1, G).

In summary, 7 days of HFD feeding caused WAT insulin resistance reflected by reductions in insulin-mediated WAT glucose uptake and suppression of WAT lipolysis.

Seven-day HFD impairs insulin-stimulated insulin signaling cascade activation in WAT

We next explored potential mechanisms by which HFD impairs insulin's suppression of WAT lipolysis by examining the components of the insulin signaling cascade that regulate the key lipolytic enzymes in epididymal WAT. Insulin-stimulated phosphorylation of both Insr and Akt were decreased in HFD-fed rats compared with RC group (Figure 2, A and B), suggesting that the defect in insulin action could be attributed to impaired Insr kinase activation. The canonical pathway by which insulin suppresses WAT lipolysis is mainly through activation of phosphodiesterase 3B (PDE3B), which then degrades cyclic adenosine monophosphate (cAMP) to halt the activation of protein kinase A (PKA)-mediated phosphorylation of lipolytic enzymes, leading to decreased activity of HSL and reduced LD protection from perilipin. Thus, we measured insulin-stimulated PDE3B phosphorylation, cAMP content and PKA activity. Rats subjected to 7-day HFD exhibited decreased insulin-stimulated phosphorylation of PDE3B, and this was associated with higher cAMP concentrations and PKA activity in WAT (Figure 2, C-E). These changes were associated with increased phosphorylation of key lipolytic proteins - adipose triglyceride lipase (ATGL) at Ser^{406}, hormone-sensitive lipase (HSL) at Ser^{660} and perilipin at Ser^{552} (Figure 2, F-H). Basal levels of these key WAT insulin signaling proteins were unchanged (Figure S2, E).

In summary, 7 days of HFD-feeding impaired insulin signaling in WAT at the level of Insr autophosphorylation limiting the ability of insulin to decrease activity of the downstream proteins involved in suppression of WAT lipolysis.

Seven-day HFD increases WAT PM *sn*-1,2-DAG content and PKCε translocation

Both HFD-induced WAT insulin resistance and hepatic insulin resistance have an insulin signaling defect at the level of IRK activation. In the liver, impaired IRK activation is attributed to activation of PKCε, and we hypothesized that a short-term HFD may also lead to activation of PKCε in WAT. As there is little data on the role of PKCs in regulating WAT physiology, we first assayed the activation of certain major PKC isoforms. Specifically, we measured translocation (from cytosol to membrane, an index of activation) of both conventional and novel PKC isoforms in WAT in RC and 7-day HFD-fed rats. The translocation and activation of PKCε, as reflected by the membrane/cytosol ratio of PKCε, increased by ~ twofold in HFD-fed rats vs. RC-fed group (Figure 2, I). In contrast, the membrane translocation of other PKC isoforms including α, β, δ and θ were unaltered by the 7-day HFD feeding (Figure S3, A-D). PKCs are activated by DAGs, specifically, *sn*-1,2-DAGs (23). DAGs are present in multiple cellular compartments, such as the ER, Mito, PM, LD and cytosol. Thus, we developed an assay to separate five subcellular compartments in WAT (Figure 2, J). Next, we measured the concentration of DAG stereoisomers in each fraction. As expected, approximately 90% of total DAG were located in the lipid droplet fraction (Figure S2, A). There were no differences in total DAG concentrations between the groups (Figure S2, B). However, we observed an approximately twofold increase in *sn*-1,2-DAGs in the PM compartment, which are mostly derived from esterification of exogeneous fatty acids into DAGs in the ER compartment (Figure 2, K). This was specifically associated with WAT PKCε membrane translocation (Figure 2, I) but not translocation of other isoforms, such as PKCα, β, δ and θ (Figure

S3, A-D). These changes occurred without evidence of adipose inflammation. Expression of genes associated with WAT inflammation and hypoxia were unchanged (Figure S3, E).

Taken together these data suggest that activation of the PKCε pathway, by a short-term HFD, is triggered by PM associated *sn*-1,2-DAGs and that the *sn*-1,2-DAG-PKCε pathway may be the primary driver leading to impaired WAT insulin signaling by short-term overnutrition.

Insr^{T1150A} mice are protected from a 7-day HFD-induced WAT insulin resistance

We had previously identified Insr Thr^{1160} as a specific residue that is phosphorylated by PKCε in the liver (6). Phosphorylation of this residue decreases the tyrosine kinase activity of Insr and downstream signaling events. Mutation of this residue from a threonine to an alanine (i.e. Insr^{T1150A}) shields Insr from this pathogenic phosphorylation and preserves hepatic insulin signaling and hepatic insulin sensitivity in HFD-fed mice. In our previous study we did not previously observe any alterations in WAT insulin action in HFD-fed Insr^{T1150A} mice (6). However, these assessments of WAT metabolism were performed during the final stages of a 140-min hyperinsulinemic-euglycemic clamp with an insulin infusion rate at 2.5 mU/(kg-min). Suppression of WAT lipolysis occurs rapidly after the onset of hyperinsulinemia (16), and the degree of WAT insulin resistance after just several days of HFD feeding is subtle and can be surmounted with higher plasma insulin concentrations. Thus, any differences in WAT lipolysis may have been obscured in our previous studies involving the Insr^{T1150A} mice.

In order to address this possibility, we performed a much shorter 30-min hyperinsulinemic-euglycemic clamp study with a lower-dose insulin infusion rate [2.0 mU/(kg-min)] to evaluate insulin action in WAT in $Insr^{T1150A}$ mice subjected to 7-day HFD. As observed previously, there were no significant differences in body composition, overnight fasting plasma glucose, insulin and NEFA concentrations as well as whole-body rates of WAT lipolysis between the WT and $Insr^{T1150A}$ group (Figure 3, A, C and E; Figure S4, A-F; Table S2). Nevertheless, $Insr^{T1150A}$ mice retained the ability of insulin to suppress WAT lipolysis as reflected by reductions in plasma NEFA concentrations, whole body glycerol turnover and fatty acid turnover (Figure 3, A-F) during the hyperinsulinemic-euglycemic clamp. In addition, WAT insulin signaling was preserved in $Insr^{T1150A}$ mice, reflected by increased insulin-stimulated Insr Tyr^{1162} phosphorylation and Akt Ser^{473} phosphorylation compared to HFD-fed WT mice (Figure 4, A and B). We also examined the impact of 7-day HFD feeding on the downstream proteins that regulate WAT lipolysis. In contrast to the WT mice subjected to 7-day HFD feeding, $Insr^{T1150A}$ mice displayed increased PDE3B activity, which subsequently resulted in reduced cAMP levels and thereby decreased PKA activity (Figure 4, C-E). Consequently, phosphorylation of perilipin, HSL and ATGL decreased in $Insr^{T1150A}$ mice (Figure 4, F-H), consistent with the preservation of insulin-mediated suppression of WAT lipolysis. These data demonstrate that phosphorylation of Insr Thr^{1160} is required for the development of WAT insulin resistance after a 7-day HFD. Taken together with our prior studies (6-15) these findings suggest that lipid-induced liver, muscle and WAT insulin resistance develop as a consequence of a common pathway involving increases in plasma membrane *sn*-1,2-DAG

content leading to PKCε activation and the consequent impairment of IRK activation due to increased Insr Thr^{1160} phosphorylation.

Discussion

Appropriate energy storage and release in healthy WAT is critical for survival under calorie scarce conditions as well as for proper nutrient distribution during feeding. Under conditions of overnutrition this process is dysregulated, especially in individuals with inherited predisposition to restrained adipocyte capacity (24). Insulin regulates energy storage in WAT, in part by suppressing lipolysis. Dysregulated WAT lipolysis (along with a decreased capacity for adipocyte expansion) could promote ectopic lipid accumulation and, consequently, insulin resistance in liver and skeletal muscle (1, 4, 25-27). Increased WAT lipolysis will also increase hepatic gluconeogenesis by providing increased delivery of glycerol and NEFA to the liver, which in turn will both promote increased gluconeogenesis (1, 16). As such, insulin's regulation of WAT lipolysis serves as a key component in the network of inter-organ communication and regulation of hepatic glucose production (1, 16). Defects in insulin's suppression of WAT lipolysis may occur early in the transition from insulin sensitivity to resistance, with defects detectable as early as 7-10 days of HFD feeding in rodents (28). This early defect precedes other well-characterized changes in the adipocytes (i.e. inflammation, hypoxia, necrosis, etc.) which in turn will also promote dysregulated WAT metabolism and increased lipolysis. The data presented here now provide a mechanistic underpinning for this phenomenon. Specifically, the PM *sn*-1,2-DAG-PKCε-Insr Thr^{1160} pathway that is responsible for lipid-induce hepatic insulin resistance, which occurs in MAFLD, may also account for lipid-induced WAT insulin resistance in the early stages of overnutrition.

Firstly, impaired WAT insulin signaling occurs rapidly during HFD feeding. We detected WAT insulin resistance after only 7 days of HFD feeding with reduced insulin-mediated WAT glucose uptake and suppression of WAT lipolysis, which was accompanied by impaired activation of key insulin signaling steps initiating at the level of IRK tyrosine auto-phosphorylation. Importantly, this subtle development of WAT insulin resistance manifests earlier than other alterations such as inflammation and hypoxia in epididymal WAT, which may predispose WAT to more severe metabolic disturbances with prolonged HFD feeding.

WAT insulin resistance can be attributed to a proximal defect in insulin signaling at the level of the Insr which ultimately impacts the regulation of key lipolytic enzymes. The defect in Insr activation leads to impaired Akt and PDE3B phosphorylation. As a consequence, the decrease in PDE3B activity permits higher concentrations of cAMP which then promotes PKA activity. PKA directly phosphorylates and activates HSL (29, 30). PKA also phosphorylates perilipin, which promotes the release of CGI58 (a key activator of ATGL) and the recruitment of HSL to the lipid droplet (31). Some have proposed that insulin may regulate WAT lipolysis in an Akt-independent pathway. Choi et al. demonstrated a noncanonical Akt-independent, phosphoinositide-3 kinase-dependent pathway regulating WAT lipolysis by selectively altering PKA targets perilipin and HSL (32). This pathway would also be impacted by the proximal defect in Insr activation and thus is consistent with our proposed model of WAT insulin resistance.

Short-term HFD feeding increases the content of *sn*-1,2-DAGs in the PM of adipocytes. Though an adipocyte is mainly comprised by a relatively massive lipid droplet, important signaling

lipids are also present in other subcellular compartments. Here we assessed the content of DAG stereoisomers in five subcellular compartments. As expected, the lipid droplet was the largest reservoir of DAGs accounting for ~90% of total DAGs. However, in epididymal WAT, there was no difference in LD *sn*-1,2-DAG content following short-term HFD feeding. In contrast, the PM DAGs account for only ~1% of total DAGs in WAT, but HFD feeding caused an approximately twofold increase in PM *sn*-1,2-DAG content.

sn-1,2-DAGs are the primary DAG product of the re-esterification pathway, while previous studies demonstrated that *sn*-2,3- and *sn*-1,3-DAGs are primarily generated through the lipolytic pathway (33). Therefore, a short-term HFD condition will likely promote more accumulation of *sn*-1,2-DAGs due to the increased flux of fatty acids into the re-esterification pathway. As for the compartment specificity, it's likely that in short-term HFD (e.g. 7-day), the other membrane compartments – ER and mitochondria have the ability to maintain a relatively steady pool of lipids, due to their relatively larger baseline lipid content or higher lipid handling capacity (oxidation or transport), while PM has a relatively small baseline lipid content and therefore is more prone to relatively large fold changes in *sn*-1,2-DAGs. In lipid droplets, DAGs mostly originate from lipolysis, and since basal rates of lipolysis do not change under this condition, DAG content in lipid droplets is not expected to change very much. However, in long-term (e.g. chronic HFD) conditions, DAG content will likely increase in the LD and potentially other subcellular compartments.

The twofold increase in PM *sn*-1,2-DAGs was associated with an approximately twofold increase in PKCε translocation and PKCε has previously been implicated to play a role in WAT

insulin action. PKCε antisense oligonucleotide treatment improved insulin-stimulated WAT glucose uptake in 3-day HFD-fed rats (5). Consistent with these results, Brandon *et al.* found that WAT-specific PKCε KO mice displayed improved glucose tolerance on HFD, indicating that WAT PKCε activation may be an essential step in the development of WAT insulin resistance (21). However there are some notable differences between the study of Brandon *et al.* and the present work. Brandon *et al.* reported that WAT-specific deletion of PKCε improved glucose tolerance in chronically HFD-fed mice, but they did not detect alterations in insulin's regulation of WAT lipolysis or insulin-stimulated glucose uptake in WAT explant after 1-week HFD. They also did not detect differences in plasma fatty acid concentrations during a glucose tolerance test. In contrast, our relatively low-dose hyperinsulinemic-euglycemic clamp studies, combined with stable isotopic measurements of lipolytic rates, provided us with a more sensitive means to detect differences in insulin regulation of WAT lipolysis in vivo.

We have previously identified Insr Thr^{1160} as a specific target that could be phosphorylated by PKCε, leading to inhibition of IRK activity in the liver (6). Phosphorylation of the Thr^{1160} residue in IRK activation loop is predicted to destabilize its active configuration, thereby inhibiting IRK activity. As such, $Insr^{T1150A}$ mice are protected from HFD-induced hepatic insulin resistance (6). WAT is exquisitely sensitive to the antilipolytic effects of insulin (34) and thus we were most likely unable to detect differences in WAT insulin action due to saturating dose of insulin administered in our prior hyperinsulinemic-euglycemic clamp studies in the $Insr^{T1150A}$ mice. In order to address this issue, we used a lower insulin infusion rate [2.0 mU/(kg-min) vs 2.5 mU/(kg-min)] for a shorter

time (30 min vs. 140 min) in the current study to better assess WAT insulin action in WT versus $Insr^{T1150A}$ mice. Under this new experimental condition, we demonstrated that $Insr^{T1150A}$ mice were protected from HFD-induced WAT insulin resistance. WAT insulin signaling was preserved at the level of IRK activity down through Akt phosphorylation, thereby preserving insulin's ability to suppress phosphorylation of perilipin, HSL and ATGL through regulating PDE3B activity and cAMP content. In summary, we demonstrated that PKCε-mediated Insr Thr^{1160} phosphorylation regulates lipid-induced WAT insulin resistance by inhibiting IRK activity.

Taken together, these data demonstrate that PM *sn*-1,2-DAG – PKCε - INSR Thr^{1160} phosphorylation is a critical pathway in the pathogenesis of short-term HFD-induced insulin resistance in WAT. Alterations in this pathway may occur during the early stage of WAT lipid over-influx, resulting in impaired insulin's regulation of WAT lipolysis and WAT glucose uptake. Though the defect in WAT is subtle, it may be a necessary predisposition to more severe WAT dysfunction as well as for ectopic lipid deposition and insulin resistance in liver and skeletal muscle in more prolonged states of overnutrition. Furthermore, given that PKCε has many additional targets in addition to INSR Thr^{1160} it is likely that PM *sn*-1,2-DAG induced PKCε activation will impact many additional targets that affect WAT metabolism independent of changes in insulin receptor kinase activity (35). Thus, longer-term studies are needed to investigate if eliminating WAT insulin resistance could abrogate other metabolic disturbances and whether these results translate to humans under conditions of short-term overnutrition and obesity. Moreover, these data identify

the PM *sn*-1,2-DAG – PKCε - INSR Thr^{1160} phosphorylation pathway as a new potential therapeutic target to treat metabolic dysfunctions that are associated with WAT insulin resistance.

Methods

Animals

All animal studies were approved by the Yale University Institutional Animal Care and Use Committee and were performed in accordance with all regulatory standards. Male Sprague-Dawley rats weighing approximately 250g were obtained from Charles River Laboratories (Wilmington, MA) and were maintained on a 12-hour light/12-hour dark cycle. After 1 week of acclimation, rats underwent surgery for placement of polyethylene catheters in the common carotid artery (PE50 tubing, Instech Solomon, Plymouth Meeting, PA) and the jugular vein (PE90 tubing, Instech), and then fed either a regular chow diet (Harlan Teklad #2018, Madison, WI; 18% calories from fat, 58% from carbohydrate, 24% from protein) or a high fat diet (Dyets #112245, Bethlehem, PA; 59% calories from fat, 26% from carbohydrate, 15% from protein), *ad lib* for 7 days.

Mice were generated and housed in the Yale Animal Resources Center under a 12-hour light/12-hour dark cycle and received ad libitum access to food and water. $Insr^{T1150A}$ mice were generated as previously reported (6). Male mice were studied at 14 to 18 weeks of age. Catheters were placed in the jugular vein 7-9 days before the hyperinsulinemia-euglycemia clamp. Mice were fed either a regular chow diet (Harlan Teklad TD2018: 18% fat, 58% carbohydrate, and 24% protein) or a high fat diet (Research Diets D12492: 60% fat, 20% carbohydrate, and 20% protein).

Hyperinsulinemic-Euglycemic Clamps

After either 7 days of regular or high-fat feeding, rats were fasted overnight. The rats underwent a basal intra-arterial prime infusion of [$^{2}H_{7}$] glucose (1.5 mg/[kg-min]), [$^{13}C_{16}$] palmitate (0.5 mg/[kg-min]) and [$^{2}H_{5}$] glycerol [1.5 mg/(kg-min)] for 5 min, followed by a continuous infusion at rate of 0.5 mg/(kg-min), 0.05 mg/(kg-min) and 0.15 mg/(kg-min) respectively for 85 min. Blood samples were taken from the jugular vein catheter at 100, 110, and 120 min of the basal infusion for measurement of lipid turnover. A short-term (30 min) hyperinsulinemic-euglycemic clamp was then conducted starting with a primed/continuous infusion of human insulin (prime 25 mU/kg-min for 5 min, 2.5 mU/kg-min) and a variable infusion of 20% dextrose to maintain euglycemia (110mg/dl approximately). Blood samples were drawn from the venous catheter at 10, 20, 30 min of the clamp, with 20 and 30min time points to measure clamp lipid turnover. Plasma insulin levels at the 90 min of basal infusion and 30 min of the clamp were measured by radioimmunoassay in the Yale Diabetes Research Center. GC/MS was used to measure plasma [$^{2}H_{5}$] glycerol and [$^{13}C_{16}$] palmitate enrichment, as we have described (16), as well as calculating rates of lipolysis by correcting for the percent fatty acids that comprises as we previously described. Glycerol and palmitate turnover was calculated as above ($Turnover = \left(\frac{Tracer\ enrichment}{Plasma\ enrichment} - 1\right) * Infusion\ rate$). Another set of 140-min clamp study was performed as previously described (5). A 200μCi bolus of 2-deoxy-[1-^{14}C]-glucose (PerkinElmer) was injected at the 120-min to monitor tissue-specific insulin-stimulated glucose uptake. For the assay of WAT glucose uptake, WAT samples were homogenized, and the supernatants were transferred to an ion-exchange column

to separate ^{14}C-2-deoxyglucose-6-phosphate from 2-deoxy-[1-^{14}C]-glucose as previously described (36). At the end of the clamp, rats were anesthetized with pentobarbital sodium (150 mg/kg), and tissues were immediately harvested and frozen with tongs in liquid N_2. Tissues and plasma were stored at -80 °C for subsequent analysis.

For the mouse clamp, study cohorts consisted of homozygous male Insr^{T1150A} mice and littermate male WT controls which were generated by our group (6). After 7 days of high-fat feeding, mice were fasted overnight. Awake mice under gentle tail restraint were first infused with [$^{13}C_{16}$]palmitate [0.3mg//(kg-min)] and [$^{2}H_{5}$]glycerol [0.075mg/(kg-min)] for 120 minutes to measure lipid turnover. A short-term (30 min) hyperinsulinemic-euglycemic clamp was then performed beginning with a primed/continuous infusion of human insulin (prime 4.8 mU/kg-min for 3 min, 2.0 mU/kg-min) and a variable infusion of 20% dextrose to maintain euglycemia (110 mg/dl approximately). At the end of the clamp, mice were anesthetized with pentobarbital sodium (150 mg/kg), and tissues were immediately harvested and snap-frozen in liquid N_2. Tissues and plasma were stored at -80 °C for subsequent analysis.

Biochemical Analysis

Plasma glucose concentrations were measured using the YSI Glucose Analyzer (Yellow Springs, OH). Plasma insulin was measured by radioimmunoassay. Plasma NEFA concentration was measured spectrophotometrically using a Wako reagent (Wako Diagnostics). cAMP was

measured by cAMP ELISA kit (Enzo Life Science) in accordance with the protocol. PKA activity was measured by PKA colorimetric activity kit (Invitrogen).

Immunoblotting and IP

WAT lysates were prepared in RIPA buffer with protease inhibitors (cOmplete MINI; Roche) and phosphatase inhibitors (PhosSTOP; Roche). Protein was measured by the BCA assay (Pierce) and equal amount of protein extraction was mixed with sample buffer containing 2% β-mercaptoethanol. After running the samples in 4% to 12% Tris-glycine gels (Novex), proteins were electrotransferred to Immobilon P PVDF membranes (Millipore) by semi-dry transfer. Membranes were blocked in 5% BSA for 1 hour at room temperature and then probed overnight at 4°C with primary antibodies. The antibodies were obtained from Cell Signaling Technology (INSR - Cat#3025, INSR pTyr^{1162} - Cat#3918, Akt - Cat#2920, Akt pSer^{473} - Cat#4060, perilipin - Cat#9349, HSL - Cat#4107, HSL pSer^{660} - Cat#4126, ATGL - Cat#2138, GAPDH - Cat#5174), abcam (ATGL pSer^{406} - Cat#ab135093, NaK-ATPase - Cat#ab7671, Calnexin - Cat#ab22595, VDAC - Cat#ab14734), Thermofisher (PDE3B – Cat#14-1973-82), FabGennix International Incorporated (pPDE3B - Cat#PPD3B-140AP), VALA Sciences (perilipin pSer^{552} - Cat#4856) and BD Biosciences (PKCε – Cat#610086). Membranes were then washed in TBS-T and incubated for 1 hour at room temperature with secondary antibodies (Cell Signaling). After washing in TBS-T for three times, antibody binding was detected by enhanced chemiluminescence (Pierce). Films

were developed within the linear dynamic range of signal intensity and then were scanned for digital analysis. Densitometry was performed using ImageJ software.

IP was performed using 1–2 mg protein from lysates prepared as described above, the lysate was incubated with antibody PDE3B (Thermo Fisher) overnight for 16 hours and then mixed with protein A/G agarose beads (Santa Cruz Biotechnology Inc.) for 4 hours. Immune complexes were washed extensively in lysis buffer and eluted in Laemmli buffer for immunoblot analysis.

PKCε translocation assay

PKCε membrane/cytosol ratio in freeze clamped WAT was assessed by western blot as previously reported (37) with slight modifications and assumed to represent PKCε activity in WAT. Briefly, 400-500mg WAT from rats fasted for 6 hours was homogenized in ice-cold buffer A containing 20 mM Tris-HCl, pH 7.4, 1 mM EDTA, 0.25 mM EGTA, 250 mM sucrose with protease inhibitors (cOmplete MINI; Roche). Lysate was centrifuged (60 min, 100,000 g, 4°C) to separate the membrane and cytosol from lipid droplet. The supernatant was saved as the cytosolic fraction. The pellet was washed once in ice-cold buffer A to remove all the lipid droplet and cytosol and then was resuspended in buffer B containing 250 mM Tris-HCl, pH 7.4, 1 mM EDTA, 0.25 mM EGTA, 2% Triton X-100 with protease inhibitors by sonication, incubated at 4°C for 45 minutes to solubilize membrane proteins, and centrifuged (60 min, 100,000 g, 4°C). The supernatant was saved as the membrane fraction. Equal amounts of protein were subjected to measure PKCε membrane/cytosol ratio by immunoblotting.

DAG Subcellular fractionation assay

Subcellular fractionation was performed as described previously (38) with modifications. 300-350mg epididymal adipose tissue were homogenized using Buffer A (250 mM sucrose–10 mM Tris (pH 7.4)–0.5 mM EDTA) in a Dounce-type tissue grinder (Kontes no. 21). All subsequent steps were performed at 4 °C. The homogenate was centrifuged at 12000 rpm in an SS-34 rotor for 15 min. The pellet was resuspended in buffer A and transferred on top of 1.12 M sucrose in a 2ml centrifuge tube. The samples were centrifuged in a TLS-55 rotor at 36,000 rpm for 20 min. The interface was transfer and diluted with buffer A, and then centrifuged in a TLA-100.2 rotor at 37,000 rpm for 9 min, the pellet was saved as plasma membrane fraction. The pellet from the previous step (TLS-55 rotor) was resuspended in buffer A and centrifuged at 12,000 rpm in an SS-34 rotor for 15 min. The pellet from this centrifugation was saved as mitochondrial membrane. The supernatant from the initial centrifuge was transferred and then centrifuged at 650000 rpm in a Ti70.1 rotor for 75 min. The pellet was saved as ER, the top layer was saved as lipid droplet and the middle layer was saved as cytosol. DAGs were extracted from the five compartmentations and measured by LC-MS/MS as described previously (28).

Statistical analysis

Comparisons were performed using the 2-tailed Student's t-test, unpaired with significance defined as a p-value<0.05. GraphPad Prism 8.0 (San Diego, CA) was used for all statistical analysis. Data are presented as the mean ± S.E.M.

Study approval

All animal studies were approved by the Yale University Institutional Animal Care and Use Committee.

Author Contributions

K.L., D.Z., V.T.S. and G.I.S. designed the experimental protocols. D.Z., K.L., J.S. and X.L. performed experiments. K.L. and D.Z. analyzed data. K.L., V.T.S. and G.I.S. wrote the manuscript with input from all co-authors.

Acknowledgments

The authors thank Ye Zhang, Jianying Dong, Xianman Zhang, Mario Kahn, Gary W. Cline, Gina Butrico, Ali R. Nasiri, Xiaoxian Ma, Wanling Zhu and Irina Smolgovsky for their excellent technical assistance. This study was supported by grants from the United States Public Health Service (R01 DK116774, R01 DK119968, R01 DK113984, P30 DK045735, R01 DK092661) and a VA Merit Award (I01 BX000901).

References

1. Petersen MC, and Shulman GI. Mechanisms of Insulin Action and Insulin Resistance. *Physiol Rev.* 2018;98(4):2133-223.
2. Carobbio S, Pellegrinelli V, and Vidal-Puig A. Adipose Tissue Function and Expandability as Determinants of Lipotoxicity and the Metabolic Syndrome. *Advances in experimental medicine and biology.* 2017;960(161-96.
3. Bodis K, and Roden M. Energy metabolism of white adipose tissue and insulin resistance in humans. *European journal of clinical investigation.* 2018;48(11):e13017.
4. Shulman GI. Cellular mechanisms of insulin resistance. *J Clin Invest.* 2000;106(2):171-6.
5. Samuel VT, Liu ZX, Wang A, Beddow SA, Geisler JG, Kahn M, Zhang XM, Monia BP, Bhanot S, and Shulman GI. Inhibition of protein kinase Cepsilon prevents hepatic insulin resistance in nonalcoholic fatty liver disease. *The Journal of clinical investigation.* 2007;117(3):739-45.
6. Petersen MC, Madiraju AK, Gassaway BM, Marcel M, Nasiri AR, Butrico G, Marcucci MJ, Zhang D, Abulizi A, Zhang XM, et al. Insulin receptor Thr1160 phosphorylation mediates lipid-induced hepatic insulin resistance. *J Clin Invest.* 2016;126(11):4361-71.
7. Lyu K, Zhang Y, Zhang D, Kahn M, Ter Horst KW, Rodrigues MRS, Gaspar RC, Hirabara SM, Luukkonen PK, Lee S, et al. A Membrane-Bound Diacylglycerol Species Induces PKC-Mediated Hepatic Insulin Resistance. *Cell Metab.* 2020;32(4):654-64 e5.
8. Yu C, Chen Y, Cline GW, Zhang D, Zong H, Wang Y, Bergeron R, Kim JK, Cushman SW, Cooney GJ, et al. Mechanism by which fatty acids inhibit insulin activation of insulin receptor substrate-1 (IRS-1)-associated phosphatidylinositol 3-kinase activity in muscle. *J Biol Chem.* 2002;277(52):50230-6.
9. Szendroedi J, Yoshimura T, Phielix E, Koliaki C, Marcucci M, Zhang D, Jelenik T, Muller J, Herder C, Nowotny P, et al. Role of diacylglycerol activation of PKCtheta in lipid-induced muscle insulin resistance in humans. *Proc Natl Acad Sci U S A.* 2014;111(26):9597-602.
10. Song JD, Alves TC, Befroy DE, Perry RJ, Mason GF, Zhang XM, Munk A, Zhang Y, Zhang D, Cline GW, et al. Dissociation of Muscle Insulin Resistance from Alterations in Mitochondrial Substrate Preference. *Cell Metab.* 2020;32(5):726-35 e5.
11. Perry RJ, Peng L, Cline GW, Wang Y, Rabin-Court A, Song JD, Zhang D, Zhang XM, Nozaki Y, Dufour S, et al. Mechanisms by which a Very-Low-Calorie Diet Reverses Hyperglycemia in a Rat Model of Type 2 Diabetes. *Cell Metab.* 2018;27(1):210-7 e3.
12. Li X, Zhang D, Vatner DF, Goedeke L, Hirabara SM, Zhang Y, Perry RJ, and Shulman GI. Mechanisms by which adiponectin reverses high fat diet-induced insulin resistance in mice. *Proc Natl Acad Sci U S A.* 2020.
13. Perry RJ, Kim T, Zhang XM, Lee HY, Pesta D, Popov VB, Zhang D, Rahimi Y, Jurczak MJ, Cline GW, et al. Reversal of hypertriglyceridemia, fatty liver disease, and insulin resistance by a liver-targeted mitochondrial uncoupler. *Cell Metab.* 2013;18(5):740-8.

14. Perry RJ, Zhang D, Zhang XM, Boyer JL, and Shulman GI. Controlled-release mitochondrial protonophore reverses diabetes and steatohepatitis in rats. *Science.* 2015;347(6227):1253-6.
15. Abulizi A, Perry RJ, Camporez JPG, Jurczak MJ, Petersen KF, Aspichueta P, and Shulman GI. A controlled-release mitochondrial protonophore reverses hypertriglyceridemia, nonalcoholic steatohepatitis, and diabetes in lipodystrophic mice. *FASEB J.* 2017;31(7):2916-24.
16. Perry RJ, Camporez JG, Kursawe R, Titchenell PM, Zhang D, Perry CJ, Jurczak MJ, Abudukadier A, Han MS, Zhang XM, et al. Hepatic acetyl CoA links adipose tissue inflammation to hepatic insulin resistance and type 2 diabetes. *Cell.* 2015;160(4):745-58.
17. Lee YS, Kim JW, Osborne O, Oh DY, Sasik R, Schenk S, Chen A, Chung H, Murphy A, Watkins SM, et al. Increased adipocyte O2 consumption triggers HIF-1alpha, causing inflammation and insulin resistance in obesity. *Cell.* 2014;157(6):1339-52.
18. Caprio S, Perry R, and Kursawe R. Adolescent Obesity and Insulin Resistance: Roles of Ectopic Fat Accumulation and Adipose Inflammation. *Gastroenterology.* 2017;152(7):1638-46.
19. Tam CS, Viardot A, Clement K, Tordjman J, Tonks K, Greenfield JR, Campbell LV, Samocha-Bonet D, and Heilbronn LK. Short-term overfeeding may induce peripheral insulin resistance without altering subcutaneous adipose tissue macrophages in humans. *Diabetes.* 2010;59(9):2164-70.
20. Alligier M, Meugnier E, Debard C, Lambert-Porcheron S, Chanseaume E, Sothier M, Loizon E, Hssain AA, Brozek J, Scoazec JY, et al. Subcutaneous adipose tissue remodeling during the initial phase of weight gain induced by overfeeding in humans. *The Journal of clinical endocrinology and metabolism.* 2012;97(2):E183-92.
21. Brandon AE, Liao BM, Diakanastasis B, Parker BL, Raddatz K, McManus SA, O'Reilly L, Kimber E, van der Kraan AG, Hancock D, et al. Protein Kinase C Epsilon Deletion in Adipose Tissue, but Not in Liver, Improves Glucose Tolerance. *Cell Metab.* 2019;29(1):183-91 e7.
22. Perry RJ, Camporez JP, Kursawe R, Titchenell PM, Zhang D, Perry CJ, Jurczak MJ, Abudukadier A, Han MS, Zhang XM, et al. Hepatic acetyl CoA links adipose tissue inflammation to hepatic insulin resistance and type 2 diabetes. *Cell.* 2015;160(4):745-58.
23. Rando RR, and Young N. The stereospecific activation of protein kinase C. *Biochem Biophys Res Commun.* 1984;122(2):818-23.
24. Lotta LA, Gulati P, Day FR, Payne F, Ongen H, van de Bunt M, Gaulton KJ, Eicher JD, Sharp SJ, Luan J, et al. Integrative genomic analysis implicates limited peripheral adipose storage capacity in the pathogenesis of human insulin resistance. *Nature genetics.* 2017;49(1):17-26.

25. Kahn BB. Adipose Tissue, Inter-Organ Communication, and the Path to Type 2 Diabetes: The 2016 Banting Medal for Scientific Achievement Lecture. *Diabetes.* 2019;68(1):3-14.
26. Saponaro C, Gaggini M, Carli F, and Gastaldelli A. The Subtle Balance between Lipolysis and Lipogenesis: A Critical Point in Metabolic Homeostasis. *Nutrients.* 2015;7(11):9453-74.
27. Vatner DF, Majumdar SK, Kumashiro N, Petersen MC, Rahimi Y, Gattu AK, Bears M, Camporez JP, Cline GW, Jurczak MJ, et al. Insulin-independent regulation of hepatic triglyceride synthesis by fatty acids. *Proc Natl Acad Sci U S A.* 2015;112(4):1143-8.
28. Cantley JL, Yoshimura T, Camporez JP, Zhang D, Jornayvaz FR, Kumashiro N, Guebre-Egziabher F, Jurczak MJ, Kahn M, Guigni BA, et al. CGI-58 knockdown sequesters diacylglycerols in lipid droplets/ER-preventing diacylglycerol-mediated hepatic insulin resistance. *Proceedings of the National Academy of Sciences of the United States of America.* 2013;110(5):1869-74.
29. DiPilato LM, Ahmad F, Harms M, Seale P, Manganiello V, and Birnbaum MJ. The Role of PDE3B Phosphorylation in the Inhibition of Lipolysis by Insulin. *Molecular and cellular biology.* 2015;35(16):2752-60.
30. Morigny P, Houssier M, Mouisel E, and Langin D. Adipocyte lipolysis and insulin resistance. *Biochimie.* 2016;125(259-66.
31. Zechner R, Zimmermann R, Eichmann TO, Kohlwein SD, Haemmerle G, Lass A, and Madeo F. FAT SIGNALS--lipases and lipolysis in lipid metabolism and signaling. *Cell Metab.* 2012;15(3):279-91.
32. Choi SM, Tucker DF, Gross DN, Easton RM, DiPilato LM, Dean AS, Monks BR, and Birnbaum MJ. Insulin regulates adipocyte lipolysis via an Akt-independent signaling pathway. *Molecular and cellular biology.* 2010;30(21):5009-20.
33. Eichmann TO, Kumari M, Haas JT, Farese RV, Jr., Zimmermann R, Lass A, and Zechner R. Studies on the substrate and stereo/regioselectivity of adipose triglyceride lipase, hormone-sensitive lipase, and diacylglycerol-O-acyltransferases. *J Biol Chem.* 2012;287(49):41446-57.
34. Kraegen EW, James DE, Jenkins AB, and Chisholm DJ. Dose-response curves for in vivo insulin sensitivity in individual tissues in rats. *The American journal of physiology.* 1985;248(3 Pt 1):E353-62.
35. Gassaway BM, Petersen MC, Surovtseva YV, Barber KW, Sheetz JB, Aerni HR, Merkel JS, Samuel VT, Shulman GI, and Rinehart J. PKCepsilon contributes to lipid-induced insulin resistance through cross talk with p70S6K and through previously unknown regulators of insulin signaling. *Proc Natl Acad Sci U S A.* 2018;115(38):E8996-E9005.
36. Youn JH, and Buchanan TA. Fasting Does Not Impaird Insulin-Stimulated Glucose Uptake But Alters Intracellular Glucose Metabolism in Conscious Rats. *Diabetes.* 1993;42(5):757-63.

37. Samuel VT, Liu ZX, Qu X, Elder BD, Bilz S, Befroy D, Romanelli AJ, and Shulman GI. Mechanism of hepatic insulin resistance in non-alcoholic fatty liver disease. *J Biol Chem.* 2004;279(31):32345-53.
38. Bogan JS, McKee AE, and Lodish HF. Insulin-responsive compartments containing GLUT4 in 3T3-L1 and CHO cells: regulation by amino acid concentrations. *Molecular and cellular biology.* 2001;21(14):4785-806.

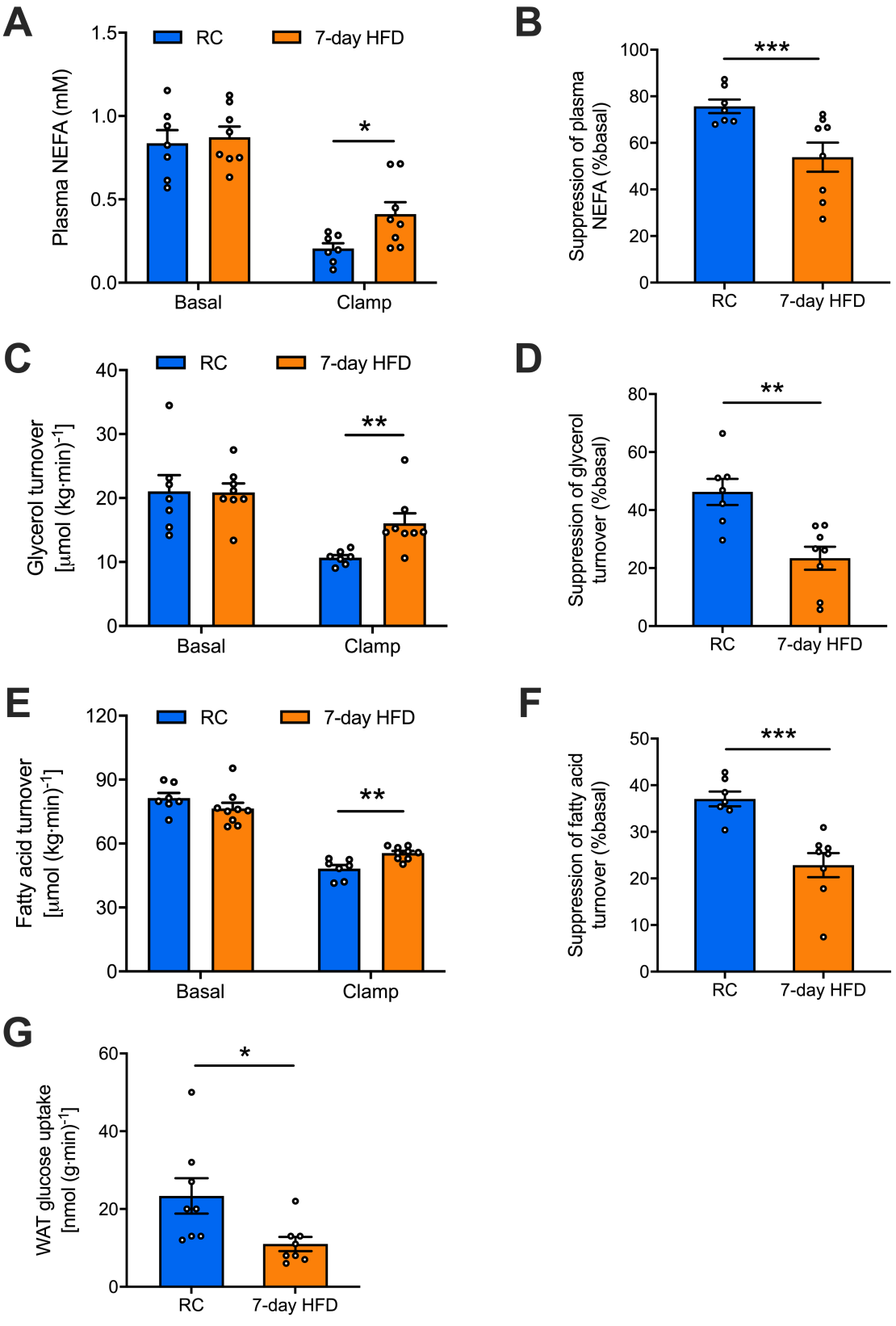
A
Plasma NEFA (mM)
1.5
1.0
0.5
0.0
RC
7-day HFD
*
Basal
Clamp
B
Suppression of plasma NEFA (%basal)
100
80
60
40
20
0
***
RC
7-day HFD
C
Glycerol turnover [µmol (kg·min)-1]
40
30
20
10
0
RC
7-day HFD
**
Basal
Clamp
D
Suppression of glycerol turnover (%basal)
80
60
40
20
0
**
RC
7-day HFD
E
Fatty acid turnover [µmol (kg·min)-1]
120
90
60
30
0
RC
7-day HFD
**
Basal
Clamp
F
Suppression of fatty acid turnover (%basal)
50
40
30
20
10
0
***
RC
7-day HFD
G
WAT glucose uptake [nmol (g·min)-1]
60
40
20
0
*
RC
7-day HFD

Figure 1. Seven-day HFD causes WAT insulin resistance reflected by reductions in WAT glucose uptake and insulin's suppression of WAT lipolysis

(A) Plasma NEFA under basal (overnight fasting) and hyperinsulinemic-euglycemic clamp conditions. (B) Insulin's suppression of plasma NEFA during the clamp. (C) and (D) Whole body glycerol turnover and its suppression by insulin during the hyperinsulinemic-euglycemic clamp. (E) and (F) Whole body fatty acid turnover and its suppression by insulin during the hyperinsulinemic-euglycemic clamp. (G) Insulin-stimulated WAT glucose uptake. In all panels, data are the mean±S.E.M. of n = 7-10 per group, with comparisons by 2-tailed unpaired Student's t-test. **P*<0.05, ***P*<0.01, ****P*<0.001.

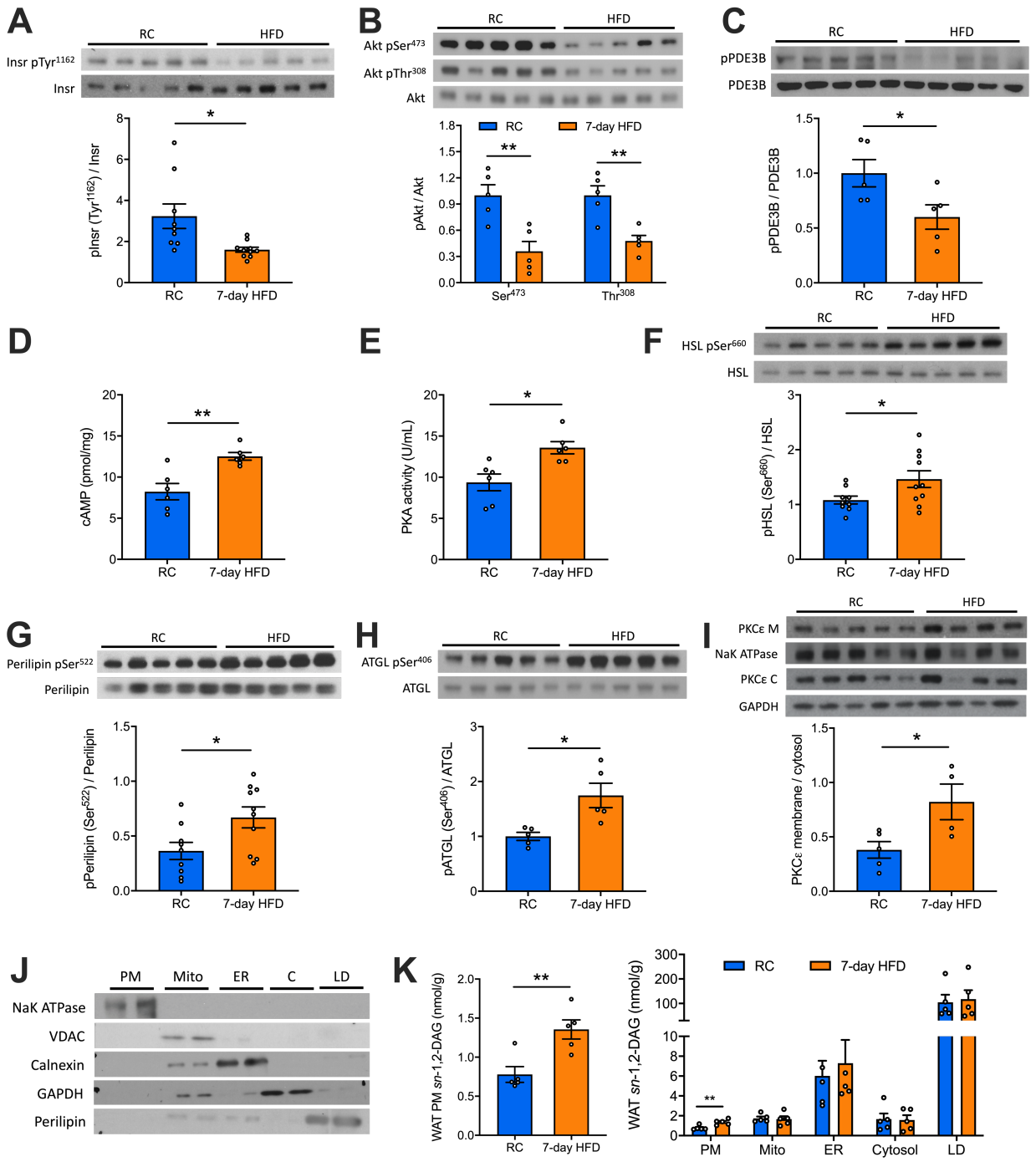
A
RC
HFD
Insr pTyr1162
Insr
pInsr (Tyr1162) / Insr
RC
7-day HFD
B
Akt pSer473
Akt pThr308
Akt
pAkt / Akt
Ser473
Thr308
C
pPDE3B
PDE3B
pPDE3B / PDE3B
D
cAMP (pmol/mg)
E
PKA activity (U/mL)
F
HSL pSer660
HSL
pHSL (Ser660) / HSL
G
Perilipin pSer522
Perilipin
pPerilipin (Ser522) / Perilipin
H
ATGL pSer406
ATGL
pATGL (Ser406) / ATGL
I
PKCε M
NaK ATPase
PKCε C
GAPDH
PKCε membrane / cytosol
J
PM
Mito
ER
C
LD
NaK ATPase
VDAC
Calnexin
GAPDH
Perilipin
K
WAT PM sn-1,2-DAG (nmol/g)
WAT sn-1,2-DAG (nmol/g)
Cytosol

Figure 2. Seven-day HFD feeding impairs insulin-stimulated insulin signaling cascade in WAT associated with increases in plasma membrane *sn*-1,2-DAGs and PKCε translocation

(A)-(C) Insulin-stimulated phosphorylation of Insr, Akt and PDE3B in WAT. (D)-(E) WAT cAMP and PKA activity during the hyperinsulinemic-euglycemic clamp. (F)-(H) Insulin-stimulated phosphorylation of HSL, perilipin and ATGL. (I) WAT PKCε membrane/cytosol ratio. (J) Separation of five subcellular compartments in WAT – plasma membrane (PM), mitochondria (Mito), endoplasmic reticulum (ER), cytosol (C) and lipid droplet (LD). (K) WAT *sn*-1,2-DAGs in five compartments. In (A)-(H) panels, rats (after overnight fasting) were under hyperinsulinemic-euglycemic clamp conditions. Data are the mean±S.E.M. of n = 5-10 per group. In (I)-(K) panels, rats were under 6-hr fasting basal condition, data are the mean±S.E.M. of n = 4-5 per group. In all panels, groups are compared by 2-tailed unpaired Student's t-test. **P*<0.05, ***P*<0.01, ****P*<0.001.

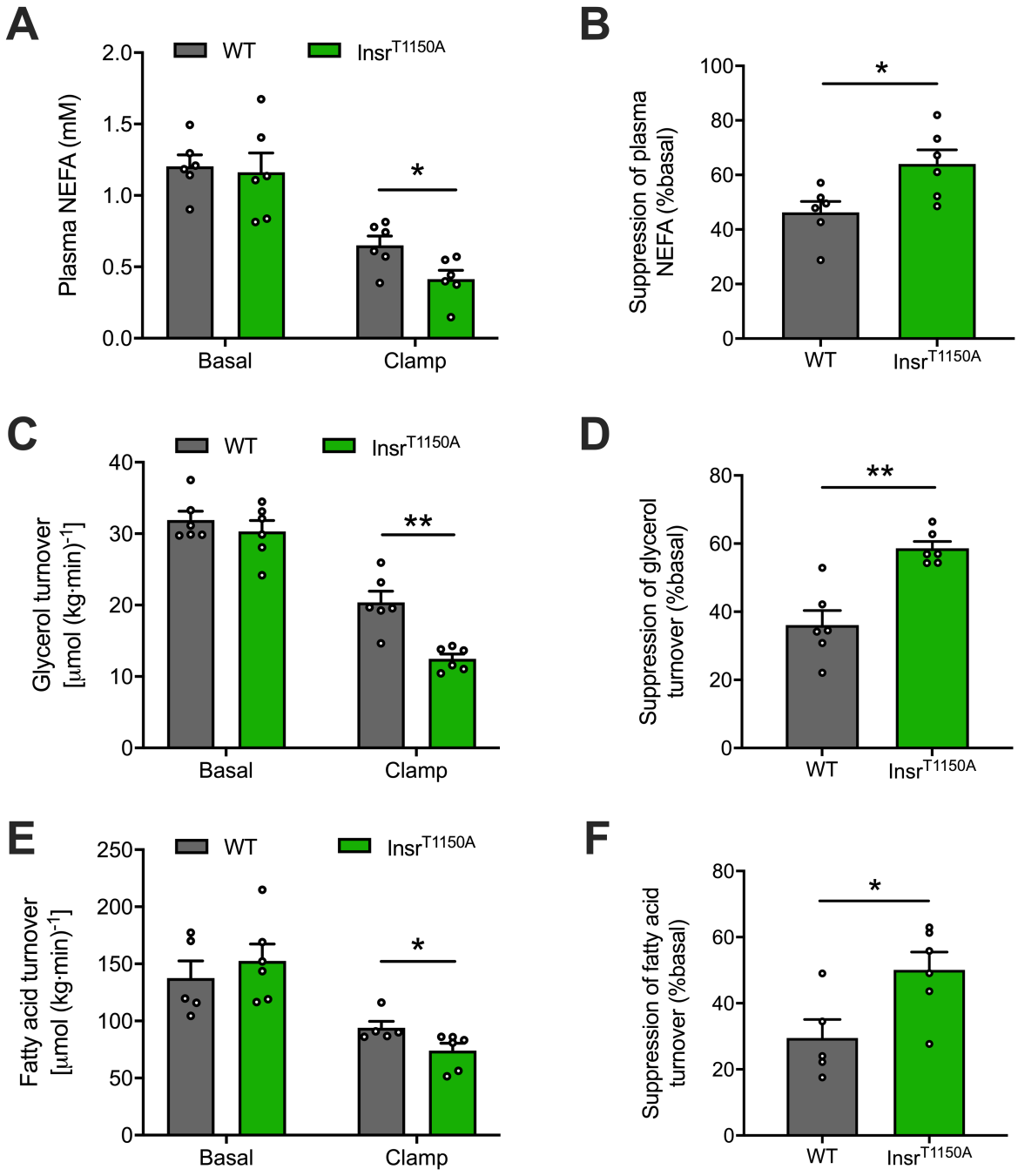
A
Plasma NEFA (mM)
2.0
1.5
1.0
0.5
0.0
WT
Insr^T1150A
*
Basal
Clamp
B
Suppression of plasma NEFA (%basal)
100
80
60
40
20
0
*
WT
Insr^T1150A
C
Glycerol turnover [µmol (kg·min)^-1]
40
30
20
10
0
WT
Insr^T1150A
**
Basal
Clamp
D
Suppression of glycerol turnover (%basal)
80
60
40
20
0
**
WT
Insr^T1150A
E
Fatty acid turnover [µmol (kg·min)^-1]
250
200
150
100
50
0
WT
Insr^T1150A
*
Basal
Clamp
F
Suppression of fatty acid turnover (%basal)
80
60
40
20
0
*
WT
Insr^T1150A

Figure 3. Insr^{T1150A} mice retain insulin's ability to suppress WAT lipolysis after 7-day HFD

(A) Plasma NEFA under basal (overnight fasting) and hyperinsulinemic-euglycemic clamp conditions. (B) Insulin's suppression of plasma NEFA during the hyperinsulinemic-euglycemic clamp. (C) and (D) Whole body glycerol turnover and its suppression by insulin during the hyperinsulinemic-euglycemic clamp. (E) and (F) Whole body fatty acid turnover and its suppression by insulin during the hyperinsulinemic-euglycemic clamp. In all panels, data are the mean±S.E.M. of n = 5-6 per group, with comparisons by 2-tailed unpaired Student's t-test. **P*<0.05, ***P*<0.01, ****P*<0.001.

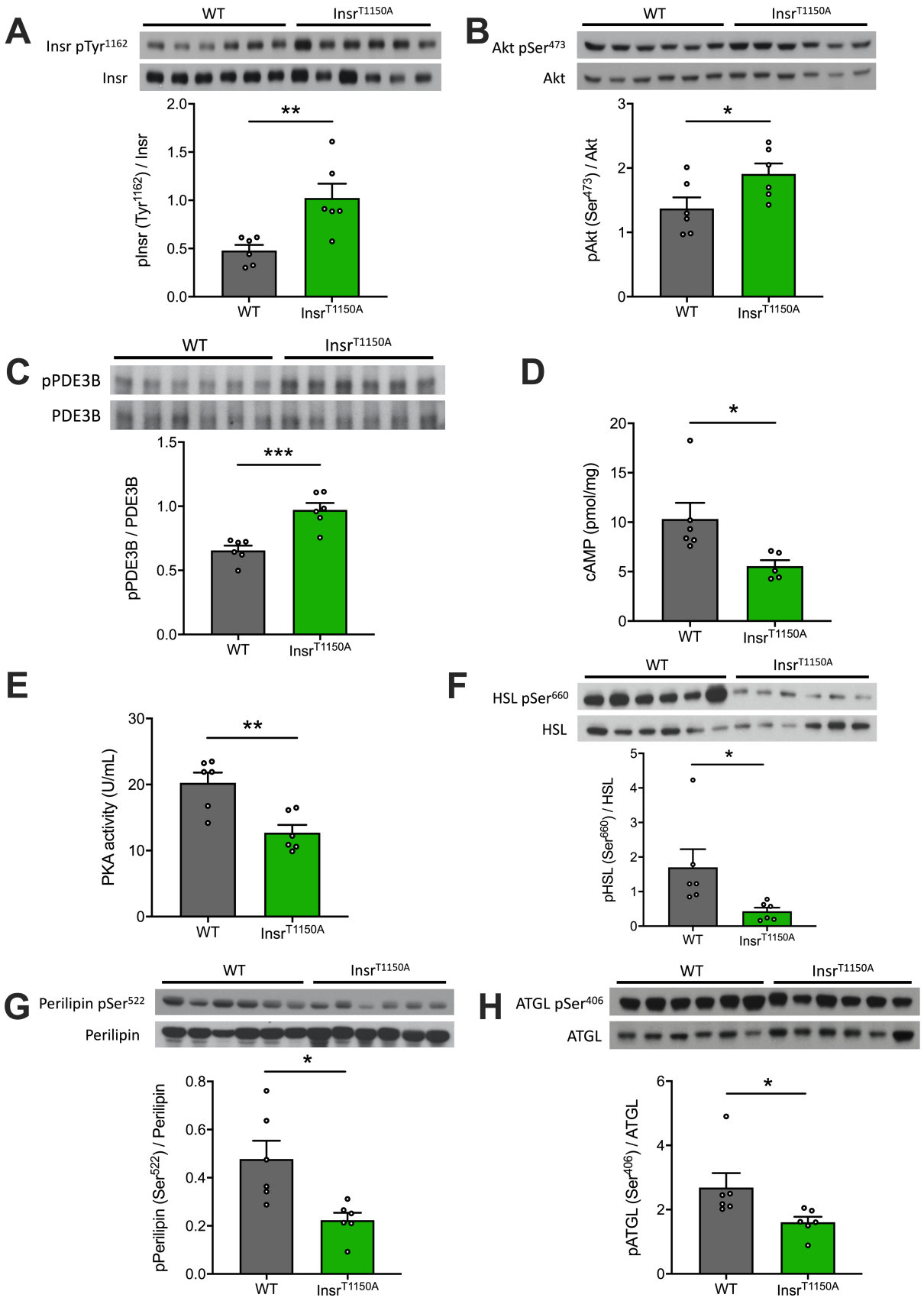
A
WT
InsrT1150A
Insr pTyr1162
Insr
pInsr (Tyr1162) / Insr
**
B
Akt pSer473
Akt
pAkt (Ser473) / Akt
*
C
pPDE3B
PDE3B
pPDE3B / PDE3B
***
D
cAMP (pmol/mg)
*
E
PKA activity (U/mL)
**
F
HSL pSer660
HSL
pHSL (Ser660) / HSL
*
G
Perilipin pSer522
Perilipin
pPerilipin (Ser522) / Perilipin
*
H
ATGL pSer406
ATGL
pATGL (Ser406) / ATGL
*

Figure 4. Insr^{T1150A} mice were protected from HFD-induced WAT insulin resistance

(A)-(C) Insulin-stimulated phosphorylation of Insr, Akt and PDE3B in WAT. (D)-(E) WAT cAMP and PKA activity during the clamp. (F)-(H) Insulin-stimulated phosphorylation of HSL, perilipin and ATGL. In all panels, mice (after overnight fasting) were under hyperinsulinemic-euglycemic clamp condition, data are the mean±S.E.M. of n = 6 per group, with comparisons by 2-tailed unpaired Student's t-test. *P<0.05, **P<0.01, ***P<0.001.